Polymer Chemistry

ROYAL SOCIETY OF CHEMISTRY

PAPER

View Article Online
View Journal | View Issue

Cite this: *Polym. Chem.*, 2024, **15**, 2081

Poly(alditol sebacate)-PLA copolymers: enhanced degradability and tunable surface properties†

Stefano Gazzotti, *[a,b] Minna Hakkarainen, [c] Carlo Andrea Pagnacco,[d] Marco Manenti, [a] Alessandra Silvani, [a,b] Hermes Farina,[a,b] Luca Arnaboldi[a,b] and Marco Aldo Ortenzi [a,b]

Received 18th March 2024,
Accepted 23rd April 2024

DOI: 10.1039/d4py00307a

rsc.li/polymers

The synthesis of aliphatic, degradable polyesters based on biobased alditols was investigated. Mannitol and dulcitol were employed as biobased building blocks for the synthesis of aliphatic polyesters in combination with sebacoyl chloride. In order to achieve optimal control over the macromolecular architecture of the polymer, multifunctional monomers were converted to bifunctional species through a straightforward protection strategy. Bifunctional di-*O*-isopropylidene derivatives were synthesized starting from mannitol and dulcitol in a one-step procedure and exploited as monomers to yield linear poly(mannitol sebacate) (PMS) and poly(dulcitol sebacate) (PDS) derivatives. The use of a bifunctional monomer allowed an optimal control over the macromolecular architecture and the synthesis of PMS and PDS-based polyols. These polyols were then employed as initiators for the synthesis of PLA-based copolymers. Two different concentrations of PMS and PDS were tested and the related effects investigated, regarding the molecular weight and thermal properties of the resulting PLA-based copolymers. Deprotection of the isopropylidene moieties on the polyol backbone was then evaluated in order to determine the influence of liberation of free OH- groups on the wettability of the materials. Finally, degradation tests were performed in different aqueous environments, showing the influence of PMS and PDS on the degradation rate of PLA-based materials.

Introduction

In pursuit of environmentally friendly materials aimed at a more sustainable future, the so-called "bioplastics" play a significant role.[1–3] Bioplastics can be either biobased or biodegradable or both[4,5] and are becoming more and more important from an industrial point of view as an alternative to oil-derived, non-biodegradable traditional plastic materials. From an environmental perspective, biobased and non-biodegradable bioplastics may have the advantage of a reduced carbon footprint with respect to their oil-derived equivalents.[6,7] However, if not properly managed, biobased materials could exhibit the same accumulation problems of their oil-derived counterparts in the environment.[8] Biodegradable plastics can offer some advantages to this regard. The best solution overall is always to properly manage and dispose of the plastic waste to end up with effective recycling. However, for all those applications in which the recovery of the end-of-life plastic is difficult or at high risk of ending up in the environment, biodegradable materials can represent a convenient solution as they could degrade to usually harmless byproducts avoiding accumulation.[9–11] However, fast degradation in all possible environments might not take place and biodegradation needs to be coupled with specific environmental conditions. In fact, some well-known biodegradable plastics, such as polylactic acid (PLA), are only certified to be degradable in industrial compost with much more harsh degradation conditions compared to natural environments. For this reason, extensive research is being carried out in the field, with both the development of completely new biodegradable materials[12] and the optimization of processing procedures of already existing ones aimed at new industrial applications.[13–17] The main issue with biodegradable plastics, however, resides in their chemical nature: biodegradability features are granted by labile bonds along the whole polymeric chain and by functional groups that are sensible to the specific conditions in which the material is expected to degrade (*i.e.* high humidity, light, heat, *etc.*).[18–20] The

[a]*Dipartimento di Chimica, Università degli Studi di Milano, Via Golgi 19, 20133 Milano, Italy. E-mail: stefano.gazzotti@unimi.it*
[b]*CRC Materiali Polimerici "LaMPo", Dipartimento di Chimica, Università degli Studi di Milano, Via Golgi 19, 20133 Milano, Italy*
[c]*Department of Fibre and Polymer Technology, KTH Royal Institute of Technology, Teknikringen 56, 100 44 Stockholm, Sweden*
[d]*Donostia International Physics Center (DIPC), Paseo Manuel Lardizabal 4, 20018 Donostia-San Sebastian, Spain.*

†Electronic supplementary information (ESI) available: NMR analyses; thermal analyses. See DOI: https://doi.org/10.1039/d4py00307a

inherent chemical weakness of these bonds therefore represents a significant hurdle for the classical processing methodologies that usually require high temperatures and mechanical stresses,[21–23] as well as for the shelf-life of the products, especially in the food packaging field.[24,25] For these reasons, it is difficult to balance properly the degradability with the mechanical and thermal properties that are required for an extended industrial applicability and including possible mechanical recyclability. Within this context, a material that, in principle, could have tuned degradability depending on the conditions appears highly valuable.

From both industrial and academic points of view, one of the most significant bioplastics is represented by the already mentioned PLA, which combines the biobased nature and biodegradability under favourable conditions with overall good properties.[26,27] For these reasons, PLA is gaining more and more importance at the industrial level and its market is steadily increasing, especially in the food packaging field.[28,29] Despite its good properties PLA biodegrades relatively slowly and lacks versatility, as it is an aliphatic polyester which, due to the standard industrial synthetic pathway, is scarcely suited for targeted chemical modifications that could be exploited to improve the desired properties.[30,31] To overcome such drawbacks, our previous works pointed out the possibility to introduce appropriate side groups through copolymerization reactions between lactide and 1,3-dioxolan-4-ones (DOX) monomers.[32–34] On a general level, copolymerization reactions can be exploited in several different ways to improve the properties of a material or a class of materials[35–39] and within this perspective, and with the idea of developing fully biobased and biodegradable materials, mannitol was investigated as a possible comonomer for the synthesis of PLA-based polyesters with tunable properties and degradability. Mannitol, dulcitol and alditol in general are biobased carbohydrates that have often been employed as monomers for the synthesis of functional polyesters.[40,41] The main hurdle for their use for this purpose is represented by their great number of functionalities that can eventually result in difficulties in controlling the macromolecular architecture and molecular weight of the final product, ultimately leading even to highly crosslinked materials. For this reason, previous reports involving the use of mannitol as a biobased monomer for the synthesis of polyesters usually deal with the protection of secondary alcohol moieties to end up with difunctional monomers.[42–45] However, these procedures rely on multi-step syntheses with overall poor yields and involvement of toxic chemicals. In this work, a single step, high yield protection strategy of mannitol and dulcitol was investigated, to synthesize difunctional di-*O*-isopropylidene-D-mannitol (i-PrMan) and di-*O*-isopropylidene-D-dulcitol (i-PrDul). Following the idea of obtaining a fully biobased material, i-PrMan and i-PrDul were combined with sebacoyl chloride to synthesize poly-mannitol sebacate (PMS) and poly-dulcitol sebacate (PDS) polyols. NMR and MALDI-TOF analyses were carried out on the PMS and PDS polyols in order to fully describe the resulting structures. These polyols were then employed as initiators for the synthesis of PLA-based materials: PLA-PMS and PLA-PDS copolymers were synthesized with different loadings of PMS and PDS, respectively. The effects of different PMS and PDS concentrations on the molecular weight and on the thermal properties of the copolymers were evaluated through SEC and TGA analyses. Wettability of the materials was also investigated, demonstrating the tunability of surface properties after deprotection of the acetals on the i-PrMan- and i-PrDul-derived units. Finally, the potential degradability of the copolymers was evaluated with "*in vitro*" studies and compared with a standard PLA synthesized under the same conditions, in order to determine the influence of the PMS and PDS cores.

Experimental

Materials and methods

Nuclear magnetic resonance (NMR). ^{1}H NMR and ^{13}C NMR spectra were recorded on Bruker Ultrashield 400 or Bruker Avance 300 MHz spectrometers at 298 K. The spectra were recorded after weighing 6 to 7 mg of sample dissolved in 0.7 mL of $CDCl_3$.

Size exclusion chromatography (SEC). The molecular weight of the synthesized polymers was evaluated using a SEC system having a Waters 1515 isocratic HPLC pump and a four Waters Styragel columns' set (HR3–HR4–HR5–HR2) with a UV Waters 2487 dual λ absorbance detector set at 230 nm, using a flow rate of 1 mL min^{-1} and 60 μL as the injection volume. The samples were prepared by dissolving 50 mg of polymer in 1 mL of anhydrous CH_2Cl_2 and filtering the solution on 0.45 μm filters. Given the relatively high loading, a check was performed using a lower concentration of polymer (5 mg mL^{-1}) in order to verify that no column overloading was observed. Higher loadings were preferred as the UV signal of PLA is relatively weak. Molecular weight data are expressed in polystyrene (PS) equivalents. The calibration was built using 16 monodispersed PS standards, having a peak molecular weight ranging from 1 600 000 Da to 106 g mol^{-1} (*i.e.* ethyl benzene). For all analyses, 1,2-dichlorobenzene was used as the internal reference. Since the SEC results are sensitive to the baseline and integration range, the molecular weights reported are approximated to the multiple of 100 Da.

Matrix-assisted laser desorption/ionization-mass spectrometry (MALDI-MS). A Bruker UltraFlex time-of-flight (TOF) mass spectrometer with a SCOUT-MTP ion source and equipped with a 337 nm nitrogen laser was used in reflector mode. Before the analysis, the samples (1 mg mL^{-1}), the matrix, DHB (10 mg mL^{-1}), and the potassium trifluoroacetate salt (1 mg mL^{-1}) solutions in MeOH were mixed and dropcast on a stainless steel MALDI plate in a volume of 8 μL.

Fourier transform infrared (FTIR) spectroscopy. FTIR spectroscopy was done on a PerkinElmer Spectrum 100 with 16 scans from 4000 to 600 cm^{-1} through a resolution of 4 cm^{-1}. The golden gate was from Graseby Specac (Kent, UK), and the software PerkinElmer Spectrum was used to process the data.

Differential scanning calorimetry (DSC). A Mettler-Toledo 820 DSC was utilized to conduct the measurements. About 5 mg of each sample was placed in a 40 μL aluminum cup with a pinhole on the lid. The applied heating rate was 10 °C min^{-1} under a nitrogen atmosphere (rate 50 mL min^{-1}). Thermal behavior was investigated using the following temperature cycles: (1) heating from 25 to 200 °C; (2) 5 min isotherm at 200 °C; (3) cooling from 200 to 25 °C; (4) 2 min isotherm at 25 °C; and (5) heating from 25 to 200 °C. The first heating and cooling cycle was run to eliminate residual internal stresses derived from the preparation. The data reported are taken from the second heating scan.

Thermogravimetric analysis (TGA). A Mettler-Toledo TGA/SDTA 851e was utilized for thermal analysis. Five milligrams of each sample were placed into a 70 μL alumina cup and heated at a rate of 10 °C min^{-1}. The measurements were performed under an 80 mL min^{-1} nitrogen flow.

Water contact angle (WCA) analyses. Surface wetting properties of the cast films were assessed by contact angle measurements using a Krüss Easydrop instrument. The contact angle values were obtained by depositing a drop (5 μL) of distilled water. Five measurements were taken on each sample to get reliable values, averaging the obtained results.

Scanning electron microscopy (SEM). An SE- 4800 SEM (Hitachi, Japan), operating at a voltage of 0.5 keV, was utilized to characterize the films. Prior to SEM observation, all samples were sputter coated with a 3.5 nm-thick Pt/Pd layer.

Synthetic procedures

Materials and methods. All chemicals were purchased from Sigma Aldrich and used as received.

Synthesis of 1,2 : 5,6-di-*O*-isopropylidene-D-mannitol (i-PrMan). i-PrMan was synthesized according to the literature procedure.[45]

Synthesis of di-*O*-isopropylidene-D-dulcitol (i-PrDul1, i-PrDul2). D-Dulcitol (100.00 g, 0.549 mol) and 2,2-dimethoxypropane (160 mL, 1.30 mol) were mechanically stirred in freshly distilled 1,2-dimethoxyethane (DME) (240 mL) at room temperature. Stannous chloride (100 mg, 0.53 mmol) was added and the reaction was warmed up to reflux for 90 min. The heat was removed and once the reaction had ceased to reflux, pyridine (240 μL) was added. The mixture was allowed to cool to room temperature and the solvent was removed under reduced pressure. The resulting crude product was redissolved in dichloromethane (600 mL) and mechanically stirred under reflux until most of the solid had dissolved. The heat was removed and once reflux had ceased, Celite (20 g) was added. The mixture was cooled to room temperature, the slurry was filtered through Celite, and the filtrate was washed with dichloromethane (2 × 100 mL). The organic washings were combined and concentrated, to provide di-*O*-isopropylidene-D-dulcitol (100 g, 80%), as a mixture of stereoisomers 1 and 2. The mixture was used without further purification. i-PrDul1: ^{1}H NMR (400 MHz, chloroform-d) δ 4.26 (td, J = 6.5, 4.7 Hz, 1H), 4.14–4.04 (m, 2H), 3.92 (dd, J = 8.6, 6.5 Hz, 1H), 3.89–3.70 (m, 3H), 3.52 (dd, J = 8.7, 4.8 Hz, 1H), 2.75 (bs, 1H), 1.50–1.35 (m, 12H). i-PrDul2: ^{1}H NMR (400 MHz, chloroform-d) δ 4.14–4.04 (m, 2H), 3.89–3.70 (m, 6H), 2.39 (s, 1H), 1.50–1.35 (m, 12H).

Synthesis of poly(mannitol sebacate) (PMS). i-PrMan (5.00 g, 19.1 mmol) and triethylamine (5.32 mL, 38.2 mmol) were stirred in anhydrous THF (30 mL) at 0 °C under a nitrogen atmosphere. Sebacoyl chloride (4.52 g, 18.9 mmol) was added dropwise. Once the addition was completed the reaction was heated to reflux and left under stirring for 16 h. The reaction mixture was then cooled to room temperature and diluted with Et_2O (150 mL). The precipitate was filtered off and the solution washed with saturated a $NaHCO_3$ solution (4 × 20 mL) and brine (4 × 20 mL). The organic phases were collected and dried over anhydrous Na_2SO_4. The solvent was evaporated under reduced pressure and PMS was recovered as a yellow highly viscous fluid.

Synthesis of poly(dulcitol sebacate) (PDS). i-PrDul (5.00 g, 19.1 mmol) and triethylamine (5.32 mL, 38.2 mmol) were stirred in anhydrous THF (30 mL) at 0 °C under a nitrogen atmosphere. Sebacoyl chloride (4.52 g, 18.9 mmol) was added dropwise. Once the addition was completed the reaction was heated to reflux and left under stirring for 16 h. The reaction mixture was then cooled to room temperature and diluted with Et_2O (150 mL). The precipitate was filtered off and the solution washed with a saturated $NaHCO_3$ solution (4 × 20 mL) and brine (4 × 20 mL). The organic phases were collected and dried over anhydrous Na_2SO_4. The solvent was evaporated under reduced pressure and PMS was recovered as a yellow highly viscous fluid.

Synthesis of PLA. L-Lactide (10 g) and tin octanoate (0.3% w/w on lactide), added as a catalyst, were introduced into a 250 mL three necked round bottomed flask. Slow nitrogen flow was used to ensure the presence of an inert atmosphere during the polymerization reaction. Mechanical stirring was provided (40 rpm). The reaction was conducted in a closed oven at 180 °C for 2 h. At the end of the reaction, the polymer was left to cool overnight under a nitrogen atmosphere.

Synthesis of PLA–polyalditol sebacate copolymers. Copolymers were synthesized by *in situ* polymerization, from L-lactide in bulk according to the following procedure. L-Lactide (10 g), PMS or PDS (5% or 10% w/w on lactide) and tin octanoate (0.3% w/w on lactide), added as a catalyst, were introduced into a 250 mL three necked round bottomed flask. Slow nitrogen flow was used to ensure the presence of an inert atmosphere during the polymerization reaction. Mechanical stirring was provided (40 rpm). The reaction was conducted in a closed oven at 180 °C for 2 h. At the end of the reaction, the polymer was left to cool overnight under a nitrogen atmosphere.

Deprotection reaction. The polymer (500 mg) was dissolved in DCM (10 mL). Anhydrous $ZnBr_2$ (50 mg, 0.22 mmol) was added and the mixture was left under stirring at room temperature for 16 h. The residual $ZnBr_2$ was then filtered off and the solution was washed with a 10% EDTA solution (3 × 20 mL). The organic phase was dried over anhydrous Na_2SO_4 and poured into a Petri dish to obtain the deprotected polymer

as a cast film. The protocol was tested on all samples (*i.e.* PLA, PLA-PMS5, PLA-PMS10, PLA-PDS5 and PLA-PDS10).

Film casting. One gram of each polymer was dissolved in 30 mL of DCM at 30 °C. Once dissolution was complete, the solutions were cast on a glass surface and the solvent was evaporated at room temperature and under pressure overnight. Film samples were then kept in a vacuum oven at 25 °C for 3 days. Complete evaporation of the solvent was checked through TGA analysis. The films were employed for the wettability tests and the SEM micrographs.

Degradation tests. Degradation tests were carried out on 300 mg of each polymer. The polymer was placed in 10 mL of four different solutions: (1) distilled water; (2) HCl solution (pH = 4); (3) NaOH solution (pH = 10) and (4) marine water solution (Instant Ocean, 37–38% salinity). Each sample was stirred for 30 days at room temperature and then the polymer was collected, dried and analysed through SEC.

Results and discussion

Monomer and polymer syntheses and structural characterization

First investigations involved the protection of mannitol. One of the most significant hurdles in the use of carbohydrate derivatives as monomers is represented by the high number of functionalities that make it difficult to target highly regular and linear structures during the polymerization. A possible solution to this problem is to selectively protect some of these free –OH groups to yield bifunctional species. Previous literature reports dealing with the protection of mannitol were aimed at the protection of the secondary alcohol moieties resulting in a bifunctional monomer with free primary hydroxyl groups.[42–44] From one side an approach of this kind can provide better reactivity since primary alcohols are, in general, less influenced by steric encumbrance. On the other hand, the selective protection of secondary alcohol moieties on alditols usually relies on multi-step procedures that are eventually troublesome and with a low overall yield. For this reason a different approach was tested, aiming at the synthesis of i-PrMan through a convenient one-step procedure, as reported in Scheme 1. The synthesis proceeded smoothly to give i-PrMan a good overall yield (80%). The protection reactions of alditols are significantly affected by their stereochemistry. For this reason, while starting from D-mannitol only one product is formed with high efficiency, the same reaction performed on D-dulcitol forms of a mixture of two distinct di-*O*-isopropylidene derivatives.[46] In this regard, the acetylation of D-dulcitol usually yields a complex mixture of products whose separation and purification may be troublesome.[47] The application of the same conditions used for the protection of mannitol to D-dulcitol yielded a mixture of two species, i-PrDul1 and i-PrDul2, as shown in Scheme 1. The composition of the mixture in terms of relative amounts of the two products was assessed through NMR. The signal relative to the two species, i-PrDul1 and i-PrDul2, can be distinguished as shown by the ^{1}H NMR expansion reported in Fig. 1. A detailed discussion of the signals' assignments is reported in the ESI.†

The comparison of the integrals of signals relative to i-PrDul1 and i-PrDul2 allowed us to determine their relative ratios as being 1 to 1.7. In order to limit the purification steps and have a direct comparison with i-PrMan, i-PrDul was employed in polymerisation as such and its reactivity was tested as a mixture of i-PrDul1 and i-PrDul2.

Both i-PrMan and i-PrDul were employed as monomers for the synthesis of polyols in the form of polyesters through combination with sebacoyl chloride.

The reaction was performed in solution, with a slight excess of i-PrMan and i-PrDul in order to target OH-terminated chains with good control. The reaction yielded polymannitol sebacate (PMS) and polydulcitol sebacate (PDS), as reported in Scheme 2. The resulting polymers were obtained as sticky, viscous products. Both PDS and PMS were analyzed by means of SEC to determine the molecular weight as well as by MALDI-TOF to assess their structural features. Molecular weight data are reported in Table 1, while MALDI-TOF ionization pattern profiles are reported in Fig. 2 and 3. As the reaction was carried out with an excess of i-PrMan and i-PrDul, both PMS and PDS were yielded as OH-terminated species, as demonstrated through MALDI-TOF analyses. MALDI-TOF and SEC analyses showed consistent results with each other. In particular, PMS was characterized by overall lower molecular

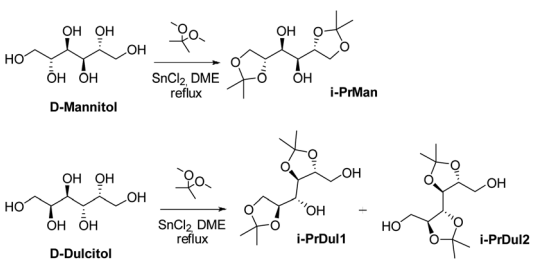

Scheme 1 Synthesis of i-PrMan and i-PrDul.

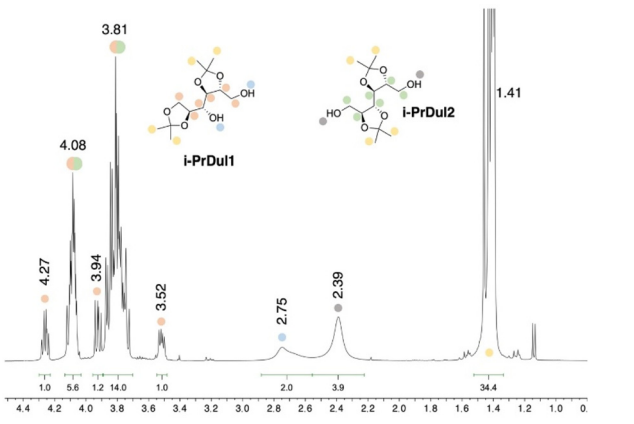

Fig. 1 Expansion of the ^{1}H NMR spectrum of i-PrDul in the 4.40–1.00 ppm region.

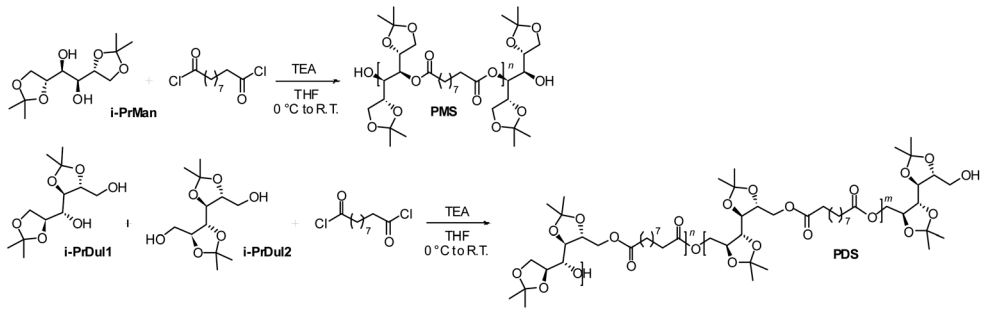

Scheme 2 Polymerization reactions of i-PrMan and i-PrDul with sebacoyl chloride to yield PMS and PDS.

Table 1 Molecular weight data for PMS and PDS

Sample	$\bar{M}_n$ [a] (g mol^{-1})	$\bar{M}_p$ [a] (g mol^{-1})	D [a]	M_w [b] (g mol^{-1})
PMS	2700	1000	6.6	2022
PDS	5300	5000	2.2	2455

[a] Determined by SEC against a PS calibration. [b] Determined as the main species in the MALDI-TOF distribution.

weight and high polydispersity, as highlighted by SEC analyses. This result is confirmed by the MALDI-TOF ionization pattern profile that shows the presence of several different distributions, likely arising from the partial reaction of the acetal side groups that results in the formation of branched polymers with complex architectures and distributions.

The main species of the three main distributions are reported in Fig. 2. On the other hand, PDS shows slightly higher molecular weights and narrower dispersity. Once again, the SEC results are confirmed by MALDI-TOF analyses, which show a well-defined distribution belonging to a linear polymeric species, as highlighted in Fig. 3. The reason for the different behavior of i-PrMan and i-PrDul may reside in their different structures, with acetal moieties less sterically hindered in the case of i-PrMan and easier to cleave.

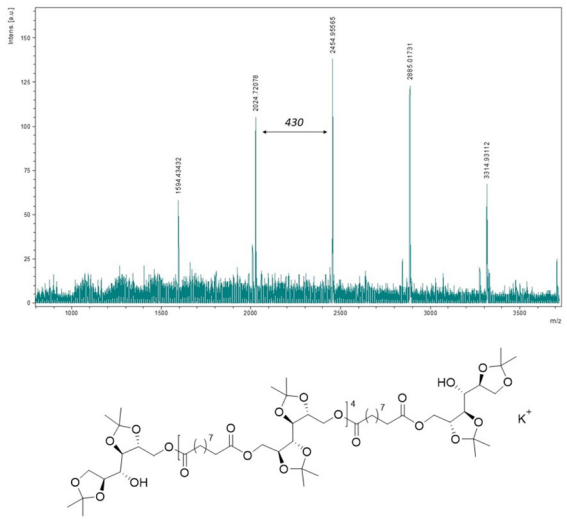

Fig. 3 MALDI-TOF spectra of PDS, with tentative assignment of the main species in the distribution.

The PMS- and PDS-based polyols were analysed by means of ^{1}H NMR spectroscopy, and the related spectra are reported in the ESI.†

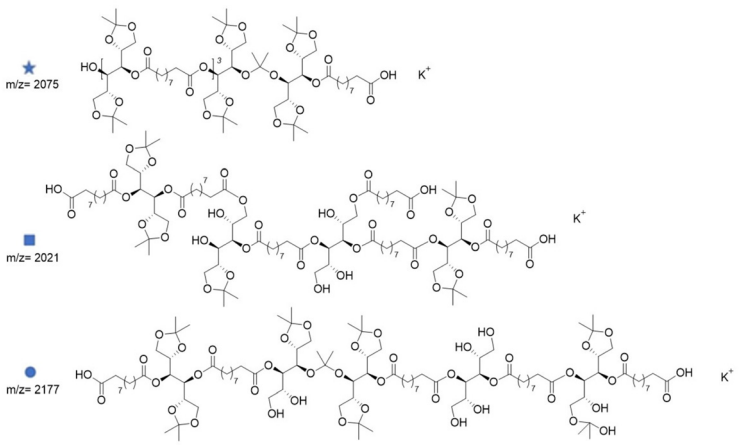

Fig. 2 MALDI-TOF spectra of PMS, with tentative assignment of the main species in each distribution.

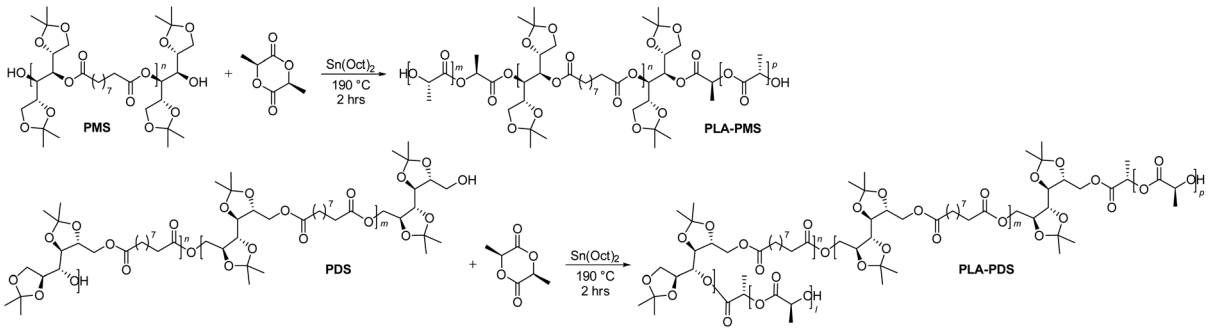

Scheme 3 Synthesis of PLA-PMS and PLA-PDS. The PLA-PMS structure has been simplified as linear.

Both these derivatives were built with the aim of using them as initiators for the ring opening polymerization of L-lactide. As the suggested structures in Fig. 2 and 3 show, both PMS and PDS have multiple OH functionalities, which could be exploited as initiators in the ring opening polymerization (ROP) reaction. In the case of the PDS the expected reaction outcome is a linear copolymer with a central PDS core and two PLA-based chain ends. PMS is expected to yield a more complex mixture of products with more complex architectures, given the higher amount of free –OH groups on each chain. The reaction was carried out under solvent-free conditions with $Sn(Oct)_2$ as the catalyst. Relying on two different loadings of PMS and PDS (5% and 10% w/w), four copolymers were synthesized, based on a central PMS or PDS core and PLA-based chain ends. The synthetic scheme is reported in Scheme 3. As already mentioned, PLA-PMS derivatives are likely characterized by complex architectures, but are simplified as linear structures in Scheme 3.

The molecular weights of the obtained copolymers were compared with standard PLA and synthesized under the same conditions (Table 2).

As the SEC data show, the molecular weight of the products is directly related to the nature and amount of polyol loaded at the beginning of the reaction. At a general level, as expected, the higher the amount of polyol, the lower the molecular weight of the final product. In addition, the molecular weight of the products appeared to be affected by the nature of the polyol. In this regard, the combination of lactide and PMS resulted in lower molecular weight products, with significantly higher polydispersity when compared to the PLA-PDS samples.

Table 2 Loading of PMS and PDS with related molecular weight

Sample	Loaded polyol (%w/w)	$\bar{M}_n{}^c$ (g mol^{--1})	$M_p{}^c$ (g mol^{--1})	D^c
PLA	0	191 800	353 800	1.9
PLA-PDS5	5[a]	81 500	109 400	2.3
PLA-PDS10	10[a]	33 900	51 500	4.0
PLA-PMS5	5[b]	45 600	69 300	6.9
PLA-PMS10	10[b]	29 500	34 500	6.0

[a] Referred to PDS. [b] Referred to PMS. [c] Determined by SEC against a PS calibration.

Also in this case the result was expected, as PMS polymer was characterized by a lower molecular weight and higher polydispersity when compared to PDS. Given the decrease of the molecular weight of the copolymers with increasing concentrations of polyol, 10% was selected as the maximum amount to be loaded.

From a chemical point of view, the differences between PDS and PMS could likely arise from the different structures of i-PrMan and i-PrDul, the latter having primary OH groups.

In order to confirm that PLA chains actually grew starting from PDS and PMS polyols, DOSY spectra were recorded. Fig. 4 reports the DOSY spectra of PLA-PDS5 and PLA-PDS10, while Fig. 5 reports the spectra of PLA-PMS5 and PLA-PMS10.

As Fig. 4 shows, both PLA-PDS5 and PLA-PDS10 were characterized by a main distribution, highlighted with green dots, alongside a secondary, lower molecular weight distribution, highlighted with red boxes. The main distribution includes signals of lactide-derived units, in blue, and signals of PDS, in yellow. This observation suggests that PLA chains were actually bonded to the PDS polyol as signals of both species were characterized by a similar diffusion. Together with the "main" PLA-PDS copolymer, both samples were also characterized by the presence of lower diffusion signals and therefore lower molecular weight species highlighted with red boxes. The species were likely responsible for the increase in

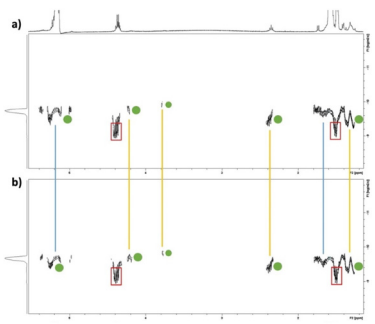

Fig. 4 DOSY spectra of (a) PLA-PDS5 and (b) PLA-PDS10. The main distribution is highlighted with green dots, while the secondary distribution is highlighted with red boxes. Signals related to lactide-derived units in the main distribution are highlighted in blue, while signals related to the PDS-derived units are highlighted in yellow.

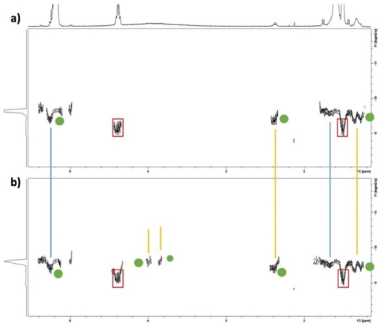

Fig. 5 DOSY spectra of (a) PLA-PMS5 and (b) PLA-PMS10. The main distribution is highlighted with green dots, while the secondary distribution is highlighted with red boxes. Signals related to lactide-derived units in the main distribution are highlighted in blue, while signals related to the PMS-derived units are highlighted in yellow.

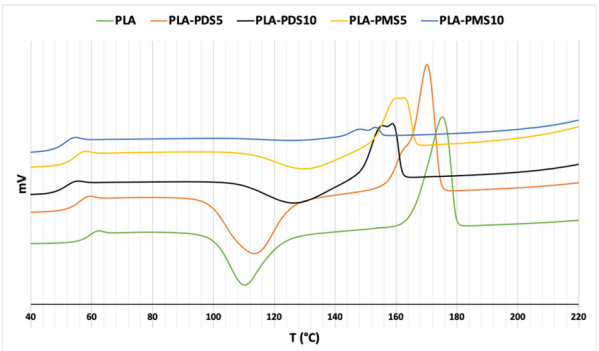

Fig. 6 Second heating scans of thermograms of the PLA and PLA-PMS and PLA-PMS copolymers.

the polydispersity of copolymers when compared to standard PLA.

Similar observations can be made for the DOSY spectra of PLA-PMS5 and PLA-PMS10, as reported in Fig. 5(a) and (b), respectively. Both samples show a main distribution characterized by the signals of both lactide- and PMS-derived units, alongside a lower molecular weight lactide-derived species. Diffusion coefficients of the different species discussed are reported in the ESI file.†

Thermal analyses

DSC analyses were carried out on all copolymers and also on the PLA sample for comparison. Glass transition (T_g), cold crystallization (T_{CC}) and melting (T_m) temperatures for each sample are reported in Table 3. Fig. 6 shows the superimposed second heating scan of the thermograms for each sample, while the cooling scans are reported in the ESI.† As the recorded thermograms show, the thermal properties of the final products were affected by the nature and amount of the loaded polyol.

The DSC results appeared to be strongly related to the macrostructure of the products as hinted by both the molecular weight data reported in Table 2 and the molecular architecture shown by MALDI-TOF. In this regard, the lower molecular weight coupled with higher polydispersity of the copolymers suggested more complex and heterogeneous materials that, in turn, have different thermal behaviours. As Fig. 6 shows, a PLA homopolymer was characterised by well-defined thermal transitions. At a general level, the addition of polyols resulted in a shift of the transitions, as well as a change in their profiles. Within this context, PLA-PDS5 showed a shift of the cold crystallization peak at higher temperatures, while the melting transition occurred at 5 °C lower with respect to the standard PLA.

These observations, together with a slight decrease of the glass transition temperatures, denounce a more amorphous character. In addition, the melting peak showed a shoulder at lower temperatures, possibly indicating the formation of a more disordered crystalline phase, probably due to some kind of polymorph. This hypothesis was confirmed by the PLA-PDS10 thermogram, where all the transitions appeared to be even more shifted when compared to both PLA and PLA-PDS5 samples.

In this regard, when compared to PLA and PLA-PDS5, the cold crystallization peak appeared to be broad and at higher temperatures, while the melting occurred at lower temperatures with a bimodal profile, as soon as cold crystallization ended. Also in this case, the observed trend was consistent with an increased structural disorder which makes the material less prone to efficient crystallization.

The PMS-loaded samples showed a similar behaviour and dependence on the amount of polyol. When compared to PLA-PDS5, PLA-PMS5 showed a more amorphous character, confirming the hypothesis of a material with less structural order, as hinted by the high polydispersity detected through SEC as well as the more complex structure shown by the MALDI-TOF analysis of PMS. Finally, PLA-PMS10 appeared to follow this trend as well, with the melting transition occurring at the lowest temperature amongst the tested samples at 153 °C, while the cold crystallization at 127 °C with a very broad peak as an indication of the limited tendency of the material to arrange in an ordered crystalline pattern. Despite being visible, the transitions were not well pronounced, denouncing an overall highly amorphous character. The reduced crystallinity of PMS-loaded copolymers can be attributed to the less ordered structures of the PMS cores when compared to PDS. The latter, despite being characterized by longer, flexible segments, presents a much more regular structure, likely resulting in a more efficient crystallization.

Table 3 DSC data for PLA, PLA-PDS and PLA-PMS copolymers

Sample	T_g[a] (°C)	T_{CC}[a] (°C)	T_m[a] (°C)
PLA	58	110	175
PLA-PDS5	54	114	170
PLA-PDS10	50	127	159
PLA-PMS5	53	130	162
PLA-PMS10	50	127	153

[a] Recorded during the second heating scan.

Deprotection

The presence of acetal moieties within the chains could be exploited to influence the properties of the final materials. In particular, a deprotection strategy was carried out in order to release the –OH groups protected as acetals coming from i-PrMan and i-PrDul. A deprotection reaction is reported in Scheme 4. Despite being labile protecting groups under acidic hydrolytic conditions, the acetal moieties in PLA-PMS and PLA-PDS derivatives have also been removed through a different experimental protocol based on the use of $ZnBr_2$. These conditions have been chosen here as they were reported to be selective on the cleavage of acetal moieties, while preserving other functionalities even in complex molecules. In the specific case of PLA-PMS and PLA-PDS copolymers, acidic hydrolytic conditions were discarded in order to avoid any possible interaction with the ester bonds within the polyester chains, likely resulting in a reduction of the molecular weight. On the other hand, acetals can be cleaved with anhydrous $ZnBr_2$, while preserving other functional groups such as esters.[48] The deprotected polymers were analysed through FTIR in order to verify the occurrence of the deprotection. In addition, ^{1}H NMR spectra were recorded to assess the deprotection through the disappearance of the methyl signals of the acetal moieties after the cleavage. The results are reported in the ESI.† WCA measurements of all polymers were then carried out, with the aim of determining whether this deprotection strategy could be applied to tune the wettability properties of the materials.

Finally, SEM analyses were performed to investigate possible phase separation phenomena triggered by the significant increase in polarity of the PMS and PDS segments after the deprotection.

FTIR analyses of polymer surfaces

FTIR analyses were performed on all the materials before and after the deprotection reaction to confirm the cleavage of the acetal moieties and the release of the OH groups alongside the PMS- and PDS-derived units. Fig. 7 reports the FTIR spectra of all four copolymers before and after the deprotection reaction.

As the spectra show, all copolymers display a significant increase of the broad band between 3600 and 3100 cm^{-1} after the treatment with $ZnBr_2$, denouncing an increase in the amount of free OH groups. This result helped to assess the occurrence of the deprotection reaction. This conclusion was further confirmed by the shift of the band towards 3600 cm^{-1}, which can be related to free OH groups. Among all the samples, PLA-PMS10 displays the smallest differences before and after the deprotection. A possible explanation could come from the uneven distribution of the phases, as highlighted in the SEM images reported in Fig. 8. The extended phase separation resulted in the formation of different areas on the surface of the materials, which could make the detection of the unprotected regions less reliable.

Wettability of polymer surfaces

Water contact angle (WCA) measurements were carried out on all polymers before and after the treatment with $ZnBr_2$, and the related results are reported in Table 4.

All protected copolymers showed a similar WCA when compared to the standard PLA, hinting the possibility of exploiting these materials in similar applications of the standard PLA, especially when specific superficial features are needed such as, for example, packaging applications. The copolymers showed a significant increase of their wettability after treatment with $ZnBr_2$, as a consequence of the removal of the acetal moieties. At the same time, the WCA of PLA remained almost constant, showing that the treatment does not affect the chemistry of the material and its surface properties.

The restoration of the free OH groups was targeted in order to demonstrate the possibility of increasing the wettability of the material on demand. As the results show, all copolymers demonstrated a significant decrease of the WCA after the deprotection, according to what was expected for a more hydrophilic surface. The most significant decrease in WCA was recorded for PDS copolymers. This observation can be attributed to the structural features of PLA-PDS copolymers as the different structures of the repeating units could contribute to a better accessibility of the OH groups by the water molecules when compared to PMS-derived units. In addition, as reported in Fig. 9, PLA-PDS10 showed phase separation phenomena after the deprotection. The uneven surface could result in a non-uniform behaviour and lower wettability when compared

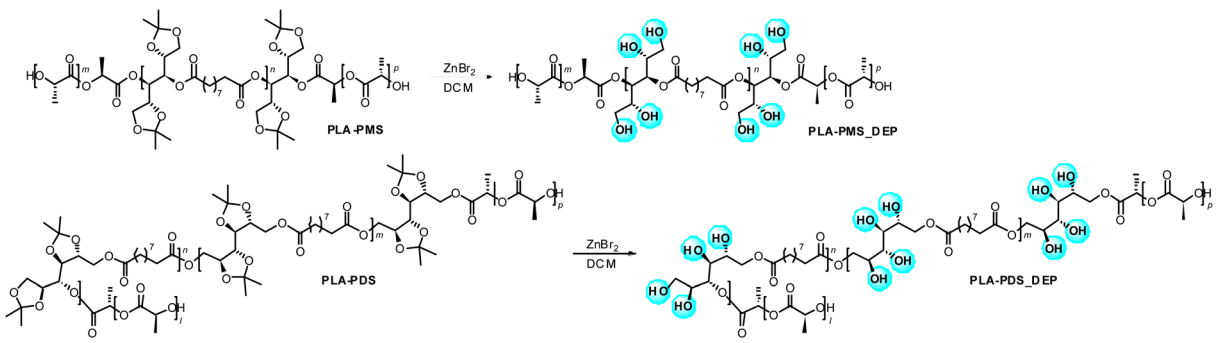

Scheme 4 The deprotection reaction on the (a) PLA-PMS and (b) PLA-PDS copolymers. The PLA-PMS structure has been simplified as linear.

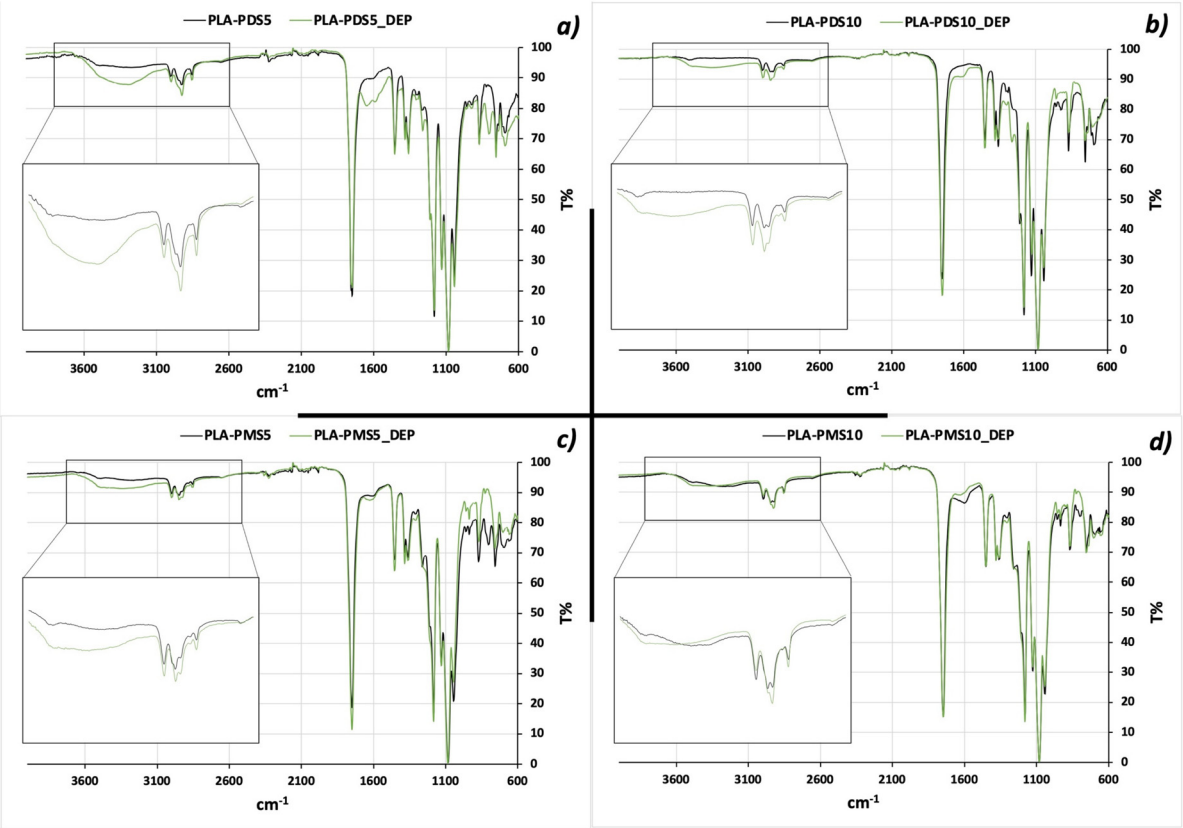

Fig. 7 Superimposed FTIR spectra of the (a) PLA-PDS5, (b) PLA-PDS10, (c) PLA-PMS5 and (d) PLA-PMS10 copolymers before and after deprotection.

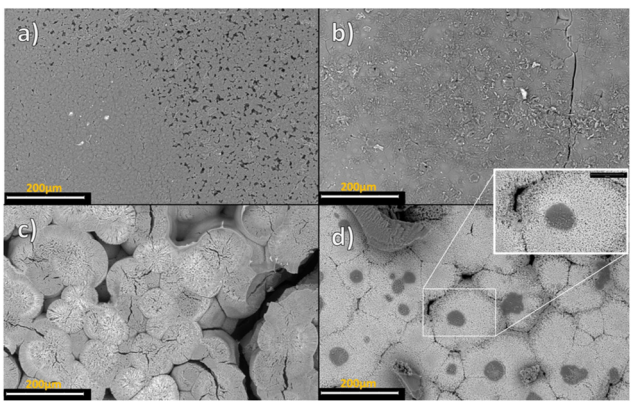

Fig. 8 SEM micrographs of (a) PLA-PDS5; (b) PLA-PDS10; (c) PLA-PDS5 after $ZnBr_2$ treatment; and (d) PLA-PDS10 after $ZnBr_2$ treatment, with magnification.

to PLA-PDS5 despite the higher concentration of PDS-derived units. As anticipated, PLA-PMS copolymers also showed an increased wettability after the deprotection, but to a lesser extent. As already discussed for PLA-PDS10, PLA-PMS10 was also characterized by phase separation phenomena both before and after the deprotection reaction.

Table 4 Water contact angle data for all the synthesized polymers before and after the treatment with $ZnBr_2$

Sample	Before $ZnBr_2$ treatment (°)	After $ZnBr_2$ treatment (°)
PLA	77 ± 3	70 ± 2
PLA-PDS5	87 ± 2	40 ± 4
PLA-PDS10	72 ± 3	44 ± 6
PLA-PMS5	67 ± 2	58 ± 4
PLA-PMS10	81 ± 4	54 ± 5

SEM images of the film surfaces

SEM analyses were performed in order to investigate surface morphology and possible phase separation phenomena, especially after deprotection, given the strong increase of polarity of the PDS and PMS-derived units. Fig. 8 shows the SEM micrographs of PLA-PDS copolymers before and after the treatment with $ZnBr_2$, while Fig. 9 shows the SEM micrographs of PLA-PMS copolymers before and after the treatment with $ZnBr_2$.

Overall, all samples showed significant differences in their appearance before and after the deprotection reaction. PLA-PDS5 and PLA-PDS10 are reported in Fig. 8a and b, respectively. The two samples show marked differences between each other, with PLA-PDS5 being characterized by better-defined spherulites as opposed to PLA-PDS10 displaying

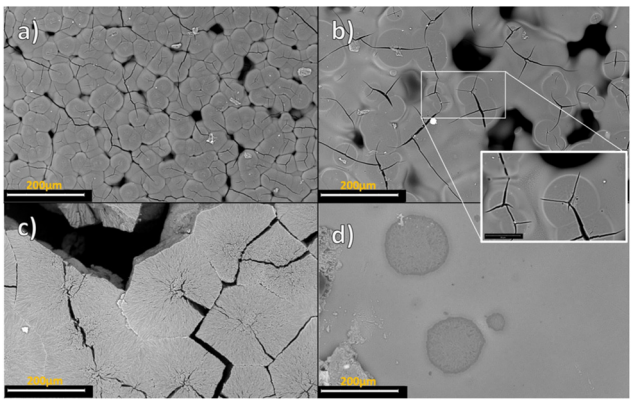

Fig. 9 SEM micrographs of (a) PLA-PMS5; (b) PLA-PMS10, with magnification; (c) PLA-PMS5 after $ZnBr_2$ treatment; and (d) PLA-PMS10 after $ZnBr_2$ treatment, with magnification.

a smoother surface. Neither of the two samples displays any visible phase separation. As anticipated, both samples showed significant differences after the treatment with $ZnBr_2$. As reported in Fig. 8c, PLA-PDS5, after the deprotection, is characterized by well-defined spherulites, with bigger sizes when compared to the material before the deprotection. Again, no phase separation was visualized. On the other hand, Fig. 8d indicates that a possible phase separation takes place after the deprotection of PLA-PDS10. Also in this case, the overall appearance of the material changed significantly, with well-defined observable spherulites after the deprotection, as opposed to the flat and uniform surface of pristine PLA-PDS10. In addition, possible phase separation was detected in the form of circular, dark areas highlighted in the magnification. Most likely, these spots are attributable to the increased polarity of the unprotected segments that may result in a reduced interaction with the PLA backbone. EDX analyses of the two areas are reported in the ESI,† showing their different chemical compositions that would confirm this hypothesis.

The PLA-PMS samples showed similar changes before and after the deprotection. As shown in Fig. 9a and c, PLA-PMS5 exhibits well-defined, round-shaped spherulites that seem to increase in dimensions after the deprotection, similar to what was observed in the case of PLA-PDS5. Also in this case, the low concentration of polyol appears to prevent phase separation phenomena even after the treatment with $ZnBr_2$. On the other hand, while PLA-PDS10 did not show signs of phase separation before the deprotection, possible phase-separated areas are visible for PLA-PMS10 as shown in Fig. 9b with related magnification. This hypothesis is confirmed by the EDX analyses of the two areas, reported in the ESI.† and showing different chemical compositions. This phenomenon is even more evident after the deprotection as shown by the round-shaped regions in Fig. 9d. As opposed to the other copolymers, the crystallites of PLA-PMS10 appear to be less evident after the deprotection, with the material characterized by a smoothened surface.

Degradation tests in water

Degradation tests in water were performed on the materials under different conditions to determine whether the presence of polyol segments could enhance their degradation rate. The tests were carried out on PLA-PDS copolymers as they demonstrated to be the most promising ones having higher molecular weights and better thermal profile and wettability features with respect to PLA-PMS copolymers. PLA was tested as well under the same conditions, to serve as a reference. Degradation behaviour was investigated in different water-based solutions, namely acidic (pH = 4), basic (pH = 10) and simulated marine. For comparison the degradation was also performed in pure distilled water. The tests were carried out with the protected copolymers; given that their overall behaviour was similar to that of the PLA used as a reference, a different degradability could provide a significant step forward in the sustainability of the materials especially when dealing with the end of life management. The samples were treated for 30 days under the different conditions and analysed afterwards by means of SEC analyses to determine if the presence of the polyol-derived units can enhance the degradability of the materials. Fig. 10a and b show the superimposed SEC curves for PLA-PDS5 and PLA-PDS10, respectively, after exposure under the different conditions. In the figures, the higher peak in the "polymer" region of the chromatogram, *i.e.* between about 1500 and 2000 seconds was normalized and given 1.0 as an absolute value. Magnifications of the low molecular weight regions are also shown to highlight the possible differences in

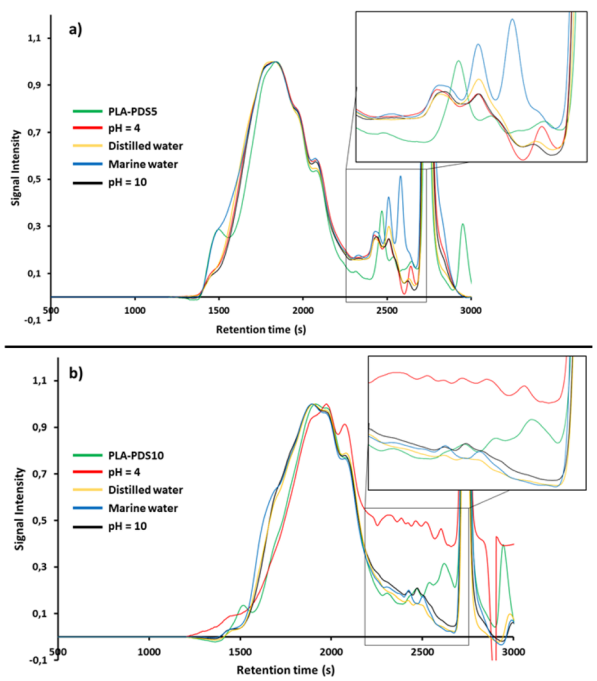

Fig. 10 (a) Superimposed SEC curves relative to PLA-PDS5 with magnification of the 2250–2750 s range. (b) Superimposed SEC curves relative to PLA-PDS10 with magnification of the 2250–2750 s range.

the distribution of the low molecular weight species that could arise from the degradation.

As Fig. 10a shows, the SEC curves related to PLA-PDS5 have similar profiles regarding the peak of the main polymeric species. Even after treatment under different conditions no significant differences are detectable, indicating that the main polymeric species is not significantly affected under the tested conditions. On the other hand, when looking at the low molecular weight region more differences are visible. In particular, while the samples treated under acidic, basic and distilled water conditions display a similar profile, the sample treated in marine water shows a higher amount of low molecular weight species. However, the degradation seems to be limited in extent as the main SEC peak is not significantly affected or shifted, but still resulting in the formation of considerable amount of low molecular weight species. This result is significant, as standard PLA is known to be quite resistant to degradation in marine water.

Fig. 10b shows the superimposed SEC curves related to PLA-PDS10. As expected, the overall profile of the curve of the polymer appears broader and more complex, in agreement with what was discussed in the previous sections. Similar to what was observed for PLA-PDS5, the profiles of the SEC curves after aging in distilled water and pH = 10 did not show significant differences with respect to the curve of pristine PLA-PDS10. In this case, the samples treated in marine water show a similar profile as well, indicating that only limited degradation took place, if any. The biggest differences reside in the sample degraded under acidic conditions. In this regard, the SEC curve was characterized both by a shift of the main peak towards longer retention times (*i.e.* lower molecular weighs), as well as the formation of a consistent number of low molecular weight species. These data show the occurrence of degradation promoted by the acidic conditions. This result is possibly connected to the labile nature of acetal moieties under acidic conditions: if they are deprotected the wettability of the material is increased and thereby its contact with the acidic medium, which accelerates further hydrolysis. In addition, the long aliphatic chains of the PDS units are likely more susceptible to acid hydrolysis with respect to the lactide-derived units.

In contrast to the copolymers, PLA showed no significant degradation under neither of the tested conditions. These results therefore appear particularly significant as different concentrations of PDS units can be exploited to affect the degradability of the materials under different conditions.

Conclusions

In conclusion, the possible applicability of mannitol and dulcitol as active monomers in the synthesis of aliphatic polyesters was demonstrated. A one-step, high yield protection strategy was put in place for obtainment of mannitol- and dulcitol-derived bifunctional monomers. These were successfully employed in the synthesis of sebacic-acid based polyesters, resulting in the formation of OH-terminated polymers. These polyols were exploited as initiators for the synthesis of PLA-based copolymers. The materials, containing different amounts of PMS and PDS, were fully characterized. The copolymers with the lowest amounts of PDS and PMS showed similar thermal properties to a standard PLA synthesized under the same conditions. This observation hints a possible range of applicability of these materials with respect to PLA. Deprotection reactions were carried out to selectively cleave the acetal moieties, which enabled tuning the wettability of the materials: after the deprotection, the materials proved to have more polar surfaces, despite some triggering of phase separation phenomena when higher concentrations of PMS or PDS were employed. Finally, the hydrolytic degradability of the PLA-PDS copolymers was tested under different aqueous conditions. PLA was included as a reference to point out possible differences promoted by the dulcitol-derived units. The two copolymers showed increased degradability under marine water and acidic conditions, appearing as promising, more degradable alternatives to PLA.

Author contributions

Stefano Gazzotti: conceptualization, formal analysis, investigation, methodology, writing – original draft, and writing – review & editing. Minna Hakkarainen: funding acquisition, project administration, resources, supervision, and validation. Carlo Andrea Pagnacco: data curation and formal analysis. Marco Manenti: data curation and formal analysis. Marco Aldo Ortenzi: methodology, project administration, writing – original draft, and writing – review & editing. Hermes Farina: investigation, methodology, and validation. Luca Arnaboldi: data curation, and formal analysis. Alessandra Silvani: data curation, supervision, and validation.

Conflicts of interest

There are no conflicts to declare.

Acknowledgements

Stefano Gazzotti gratefully acknowledges the financial support from the Foundation BLANCEFLOR Boncompagni-Ludovisi, ńee Bildt.

References

1 A. Nandakumar, J. A. Chuah and K. Sudesh, Bioplastics: A boon or bane?, *Renewable Sustainable Energy Rev.*, 2021, **147**, 111237.
2 S. Nanda, B. R. Patra, R. Patel, J. Bakos and A. K. Dalai, Innovations in applications and prospects of bioplastics

and biopolymers: a review, *Environ. Chem. Lett.*, 2022, **20**, 379–395.
3 A. Di Bartolo, G. Infurna and N. D. Dintcheva, A Review of Bioplastics and Their Adoption in the Circular Economy, *Polymers*, 2021, **13**, 1229.
4 M. Vert, Y. Doi, K. H. Hellwich, M. Hess, P. Hodge, P. Kubisa, M. Rinaudo and F. Schué, Terminology for biorelated polymers and applications (IUPAC Recommendations 2012), *Pure Appl. Chem.*, 2012, **84**, 377–410.
5 European Bioplastics, **https://www.european-bioplastics.org/bioplastics/**.
6 F. M. Lamberti, L. A. Román-Ramírez and J. Wood, Recycling of Bioplastics: Routes and Benefits, *J. Polym. Environ.*, 2020, **28**, 2551–2571.
7 M. H. Rahman and P. R. Bhoi, An overview of non-biodegradable bioplastics, *J. Cleaner Prod.*, 2021, **294**, 126218.
8 S. Gazzotti, B. De Felice, M. A. Ortenzi and M. Parolini, Approaches for Management and Valorization of Non-Homogeneous, Non-Recyclable Plastic Waste, *Int. J. Environ. Res. Public Health*, 2022, **19**(16), 10088.
9 S. M. Emadian, T. T. Onay and B. Demirel, Biodegradation of bioplastics in natural environments, *Waste Manage.*, 2017, **59**, 526–536.
10 V. Bátori, D. Åkesson, A. Zamani, M. J. Taherzadeh and I. S. Horváth, Anaerobic degradation of bioplastics: A review, *Waste Manage.*, 2018, **80**, 406–413.
11 E. M. N. Polman, G. M. Gruter, J. R. Parsons and A. Tietema, Comparison of the aerobic biodegradation of biopolymers and the corresponding bioplastics: A review, *Sci. Total Environ.*, 2021, **753**, 141953.
12 A. Costa, T. Encarnação, R. Tavares, T. T. Bom and A. Mateus, Bioplastics: Innovation for Green Transition, *Polymers*, 2023, **15**, 517.
13 N. Ehman and M. C. Area, Bioplastics are revolutionizing the packaging industry, *BioResources*, 2021, **16**, 4663–4666.
14 H. Yue, Y. Zheng, P. Zheng, J. Guo, J. P. Fernández-Blázquez, J. H. Clark and Y. Cui, On the improvement of properties of bioplastic composites derived from wasted cottonseed protein by rational cross-linking and natural fiber reinforcement, *Green Chem.*, 2020, **22**, 8642.
15 H. Kim, S. Lee, Y. Ahn, J. Lee and W. Won, Sustainable Production of Bioplastics from Lignocellulosic Biomass: Technoeconomic Analysis and Life-Cycle Assessment, *ACS Sustainable Chem. Eng.*, 2020, **8**, 12419–12429.
16 N. I. Ibrahim, F. S. Shahar, M. T. H. Sultan, A. U. M. Shah, S. N. A. Safri and M. H. M. Yazik, Overview of Bioplastic Introduction and Its Applications in Product Packaging, *Coatings*, 2021, **11**, 1423.
17 X. Zhao, K. Cornish and Y. Vodovotz, Narrowing the Gap for Bioplastic Use in Food Packaging: An Update, *Environ. Sci. Technol.*, 2020, **54**, 4712–4732.
18 J. S. Jaworska, R. S. Boethling and P. H. Howard, Recent developments in broadly applicable structure– biodegradability relationships, *Environ. Toxicol. Chem.*, 2003, **22**, 1710–1723.
19 S. Chinaglia, M. Tosin and F. Degli-Innocenti, Biodegradation rate of biodegradable plastics at molecular level, *Polym. Degrad. Stab.*, 2018, **147**, 237–244.
20 R. S. Boethling, P. H. Howard, W. Meylan, W. Stiteler, J. Beauman and N. Tirado, Group Contribution Method for Predicting Probability and Rate of Aerobic Biodegradation, *Environ. Sci. Technol.*, 1994, **28**, 459–465.
21 V. K. Rangari, R. Samsur and S. Jeelani, Mechanical, Thermal, and Electrical Conducting Properties of CNTs/Bio-Degradable Polymer Thin Films, *J. Appl. Polym. Sci.*, 2013, 1249.
22 B. K. Chen, C. C. Shih and A. F. Chen, Ductile PLA nanocomposites with improved thermal stability, *Composites, Part A*, 2012, **43**, 2289–2295.
23 F. Carrasco, D. Dionisi, A. Martinelli and M. Majone, Thermal Stability of Polyhydroxyalkanoates, *J. Appl. Polym. Sci.*, 2006, **100**, 2111–2121.
24 M. Zhang, G. M. Biesold, W. Choi, J. Yu, Y. Deng, C. Silvestre and Z. Lin, Recent advances in polymers and polymer composites for food packaging, *Mater. Today*, 2022, **53**, 134.
25 V. Siracusa, P. Rocculi, S. Romani and M. Dalla Rosa, *Trends Food Sci. Technol.*, 2008, **19**, 634–643.
26 A. Djukić-Vuković, D. Mladenović, J. Ivanović, J. Pejinb and L. Mojović, Towards sustainability of lactic acid and poly-lactic acid polymers production, *Renewable Sustainable Energy Rev.*, 2019, **108**, 238–252.
27 T. P. Haider, C. Volker, J. Kramm, K. Landfester and F. R. Wurm, Plastics of the Future? The Impact of Biodegradable Polymers on the Environment and on Society, *Angew. Chem., Int. Ed.*, 2019, **58**, 50–62.
28 M. Cvek, U. C. Paul, J. Zia, G. Mancini, V. Sedlarik and A. Athanassiou, Biodegradable Films of PLA/PPC and Curcumin as Packaging Materials and Smart Indicators of Food Spoilage, *ACS Appl. Mater. Interfaces*, 2022, **14**, 14654–14667.
29 T. Angelin Swetha, A. Bora, K. Mohanrasu, P. Balaji, R. Raja, K. Ponnuchamyd, G. Muthusamye and A. Arun, A comprehensive review on polylactic acid (PLA) – Synthesis, processing and application in food packaging, *Int. J. Biol. Macromol.*, 2023, **234**, 123715.
30 T. Fuoco, A. Finne-Wistrand and D. Pappalardo, A Route to Aliphatic Poly(ester)s with Thiol Pendant Groups: From Monomer Design to Editable Porous Scaffolds, *Biomacromolecules*, 2016, **17**, 1383–1394.
31 W. Ren, Z. Li, Y. Chen, H. Gao, W. Yang, Y. Wang and Y. Luo, Facile Preparation of Linear Polyurethane from UPy-Capped Poly(dl-Lactic Acid) Polyol, *Macromol. Mater. Eng.*, 2019, **304**, 1800491.
32 S. Gazzotti, M. A. Ortenzi, H. Farina and A. Silvani, Synthesis of Fluorine-Containing, UV-Responsive PLA-Based Materials by Means of Functionalized DOX Monomer, *Macromol. Chem. Phys.*, 2022, **223**, 2100436.
33 S. Gazzotti, K. H. Adolfsson, M. Hakkarainen, H. Farina, A. Silvani and M. A. Ortenzi, DOX mediated synthesis of PLA-co-PS graft copolymers with matrix-driven self-assem-

bly in PLA-based blends, *Eur. Polym. J.*, 2022, **170**, 111157.

34 S. Gazzotti, M. A. Ortenzi, H. Farina, M. Disimino and A. Silvani, Carvacrol- and Cardanol-Containing 1,3-Dioxolan-4-ones as Comonomers for the Synthesis of Functional Polylactide-Based Materials, *Macromolecules*, 2020, **53**, 6420–6431.

35 M. A. Ortenzi, S. Gazzotti, B. Marcos, S. Antenucci, S. Camazzola, L. Piergiovanni, H. Farina, G. Di Silvestro and L. Verotta, Synthesis of Polylactic Acid Initiated through Biobased Antioxidants: Towards Intrinsically Active Food Packaging, *Polymers*, 2020, **12**, 1183.

36 Y. Zheng and P. Pan, Crystallization of biodegradable and biobased polyesters: Polymorphism, cocrystallization, and structure-property relationship, *Prog. Polym. Sci.*, 2020, **109**, 101291.

37 H. Xu, J. Zhou, K. Odelius, Z. Guo, X. Guan and M. Hakkarainen, Nanostructured Phase Morphology of a Biobased Copolymer for Tough and UV-Resistant Polylactide, *ACS Appl. Polym. Mater.*, 2021, **3**, 1973–1982.

38 C. Chen, Y. Tian, F. Li, H. Hu, K. Wang, Z. Kong, W. B. Ying, R. Zhang and J. Zhu, Toughening Polylactic Acid by a Biobased Poly(Butylene 2,5- Furandicarboxylate)–b–Poly(Ethylene Glycol) Copolymer: Balanced Mechanical Properties and Potential Biodegradability, *Biomacromolecules*, 2021, **22**, 374–385.

39 L. Fournier, D. M. Rivera Mirabal and M. A. Hillmyer, Toward Sustainable Elastomers from the Grafting-Through Polymerization of Lactone-Containing Polyester Macromonomers, *Macromolecules*, 2022, **55**, 1003–1014.

40 K. M. Ziaa, A. Noreena, M. Zubera, S. Tabasuma and M. Mujahid, Recent developments and future prospects on bio-based polyesters derived from renewable resources: A review, *Int. J. Biol. Macromol.*, 2016, **82**, 1028–1040.

41 A. Sonseca, O. Menes and E. Gimenez, A comparative study of the mechanical, shape- memory, and degradation properties of poly(lactic acid) nanofiber and cellulose nanocrystal reinforced poly(mannitol sebacate) nanocomposites, *RSC Adv.*, 2017, **7**, 21869.

42 C. Lavilla, A. Martínez de Ilarduya, A. Alla and S. Muñoz-Guerra, PET copolyesters made from a D-mannitol-derived bicyclic diol, *Polym. Chem.*, 2013, **4**, 282.

43 C. Lavilla, A. Martínez de Ilarduya, A. Alla, M. G. García-Martín, J. A. Galbis and S. Muñoz-Guerra, Bio-Based Aromatic Polyesters from a Novel Bicyclic Diol Derived from D–Mannitol, *Macromolecules*, 2012, **45**, 8257–8266.

44 C. Lavilla, A. Alla, A. Martínez de Ilarduya and S. Muñoz-Guerra, High Tg Bio-Based Aliphatic Polyesters from Bicyclic D–Mannitol, *Biomacromolecules*, 2013, **14**, 781–793.

45 K. Hashimoto, N. Hashimoto, T. Kamaya, J. Yoshioka and H. Okawa, Synthesis and Properties of Bio-Based Polyurethanes Bearing Hydroxy Groups Derived from Alditols, *J. Polym. Sci., Part A: Polym. Chem.*, 2011, **49**, 976–985.

46 E. L. Borges, M. T. Ignasiak, Y. Velichenko, G. Perin, C. A. Hutton, M. J. Davies and C. H. Schiesser, Synthesis and Antioxidant Capacity of Novel Stable 5- Tellurofuranose Derivatives, *Chem. Commun.*, 2018, **54**, 2990–2993.

47 J. F. Chittenden, Acetalation studies. Part VII. Some new aspects of the isopropylidenation of galactitol, *Recl. Trav. Chim. Pays-Bas*, 1989, **108**, 14–19.

48 C. Ribes, E. Falomir and J. Murga, Selective cleavage of acetals with $ZnBr_2$ in dichloromethane, *Tetrahedron*, 2006, **62**, 1239–1244.